A 27.5dBm EIRP D-Band Transmitter Module on a Ceramic Interposer

Ali A. Farid, Ahmed S. H. Ahmed, Mark J. W. Rodwell
ECE Department, University of California Santa Barbara, USA
afarid@ece.ucsb.edu

***Abstract*—We present a fully packaged D-band direct conversion transmitter module on a low-permittivity ceramic carrier (Kyocera GL771, $\varepsilon_r = 5.2, \delta = 0.003$). The module has a broadband 135GHz 22FDX CMOS direct conversion transmitter, a medium-power (100mW P_{sat}) high-efficiency power amplifier implemented in Teledyne 250nm InP HBT technology, and a series-fed microstrip patch antenna array. The CMOS IC is flip-chip bonded to the carrier using 50 μm diameter copper studs, while the InP IC is wire bonded, with impedance-matching networks on the carrier compensating for the wire bonds' parasitic impedances. The module has 6GHz 3-dB modulation bandwidth and 27.5dBm measured effective isotropic radiated power (EIRP) at saturation. Under 5Gbaud, 64QAM modulation (30Gbps), the module shows 8.5% RMS error vector magnitude (EVM) at 21.5dBm EIRP. To our knowledge, the module has the highest reported EIRP and efficiency among D-band single channel transmitters.**

***Keywords*— Heterogeneously integrated transmitters, D-band transmitter, D-band InP Power amplifiers, millimeter wave packaging, Ceramic interposers, LTCC carrier, D-band antenna.**

I. Introduction

The wide mm-wave spectrum between 100GHz and 300GHz can be exploited to build very high capacity wireless communication systems. Advances in CMOS and III-V IC technologies now enable high-performance transceivers at such frequencies [1-3]. Moderate to high transmitter EIRP is necessary to overcome high atmospheric and λ^2/R^2 losses, while high-volume applications demand low-cost, high-performance packaging. Reported results include a 142-157GHz GaAs mHEMT transmitter on silica substrate with 8dBm P_{sat} and 3.5dB measured packaging loss [2], a 135-170GHz SiGe BiCMOS transmitter on a glass interposer with 13dBm peak output power and 1dB packaging loss [3], and a 94GHz heterogeneously integrated InP HBT/CMOS transmitter with 16dBm P_{sat} and unstated transition losses [4].

Here we present a D-band transmitter module using 22nm FDSOI CMOS and 250nm InP HBT ICs packaged on a low-permittivity low-temperature-cofired ceramic (LTCC) carrier. The module has an integrated 8-element series-fed patch antenna with 11dB gain and 6GHz 3-dB bandwidth. The module has 27.5dBm measured EIRP 6-GHz 3-dB modulation bandwidth. Testing the transmitter module using a commercial D-band receiver, under 5Gbaud, 64QAM modulation (30Gbps), the module shows 8.5% RMS error vector magnitude (EVM) at 21.5dBm EIRP

II. Transmitter Module Design and Integration

The CMOS (GlobalFoundries 22nm FDSOI) direct conversion transmitter IC has 2.8dBm saturated output power, with a similar performance to previous research work of [1]. It is bonded to the carrier using 50μm diameter copper pillars. The CMOS IC drives an InP HBT power amplifier (Teledyne 250nm InP HBT) having 20.5dBm P_{sat} and 20% peak PAE, which has similar performance as previous research of [5]. The InP PA is attached to the carrier using silver-filled epoxy (84-1LMISNB), while its input, output and power supplies are connected to the carrier using 1mil diameter Au wire bonds. The PA output is connected to an 8-element, series-fed patch antenna on the carrier (Fig 1).

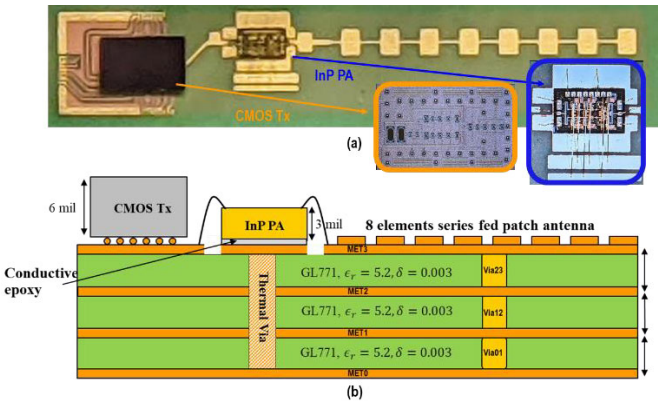

Fig. 1. D-band transmitter module (a) micrograph and (b) schematic cross-section.

The LTCC carrier (Kyocera GL771) has 3 dielectric layers, each with $\varepsilon_r = 5.2, \delta = 0.003$, and 4 metal layers. The dielectric constant is relatively low for LTCC, reducing skin-effect and substrate dielectric mode coupling losses in transmission-lines and antennas. The top metal layer (MET3) forms the antenna and microstrip signal lines routing the mm-wave, I/Q baseband, and LO reference signals. MET2 and MET0 serve as ground planes, while MET1 routes supply and bias voltages. Thermal vias are placed below the InP IC to reduce the PA's operating temperature and thereby avoid degrading its output power.

A. InP PA housing in the ceramic carrier

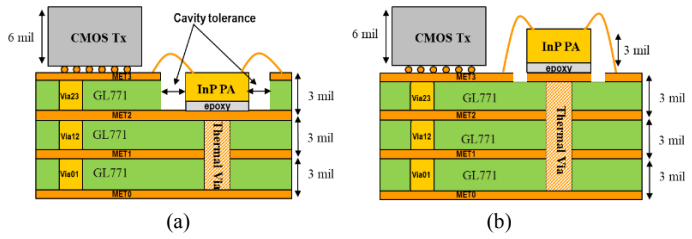

Fig. 2. Power amplifier mounting in the ceramic carrier (a) with cavity and (b) without cavity.

Wire bond parasitics will reduce the PA gain and the power it delivers to the antenna. The PA can be either mounted within a cavity (Fig. 2a) or on the LTCC top surface (Fig. 2b). While cavity mounting avoids the 3mil bond wire height difference associated with the thickness of the InP die, the +/-150µm (6mil) lateral tolerance in the cavity dimensions increases the necessary lateral distance spanned by the wire bond. Surface mounting ultimately allowed a shorter bond, and hence was selected. The minimum wire bond length is set by the PA die thickness and by the amount of lateral extrusion of the die-attach epoxy from under the IC.

B. CMOS/ InP PA transition design

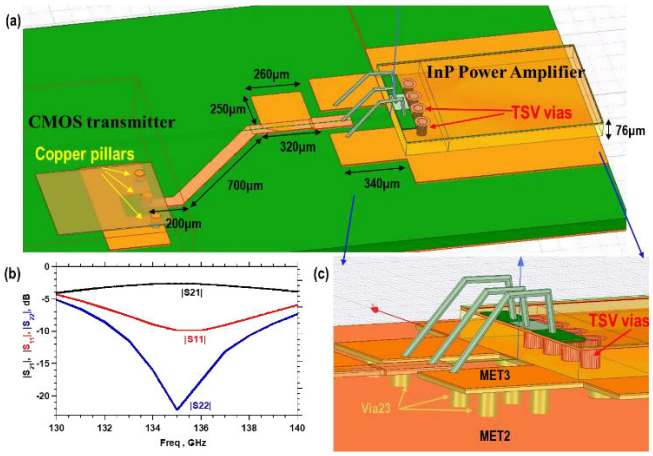

Fig. 3. CMOS transmitter to InP transition design (a) Impedance matching network on HFSS (b) Matching network S-parameters (c) InP-LTCC transition

The PA input wire bonds (Fig. 3a) are Au with 150µm length and 1-mil diameter. Though InP-LTCC bonds are provided for both signal and ground, the ground bonds have only minor effect, as the RF ground-return currents on the LTCC MET2 ground plane, after passing through the LTCC MET2-MET3 vias, mainly pass through MET3 (Fig. 3c) to the InP IC back surface, and then through InP through-substrate vias (TSV's) to the InP IC top surface ground plane. A network (Fig. 3a) on the LTCC carrier compensates for the wire bond parasitics, matching the PA input to the CMOS 50Ω output impedance. The network has 2.6dB simulated insertion loss at 135GHz (Fig. 3b), including the loss from the wire bond, the ~1mm total interconnect length, and the CMOS copper pillars (30µm height and 50µm diameter). The network has 8GHz 1-dB bandwidth.

C. InP PA to Series Fed Patch Antenna design

The eight-element series-fed patch antenna, designed using Ansys HFSS, was matched (Fig. 4a) to the InP PA output, including the wire-bonds, using a stepped-impedance transmission line. The simulated antenna gain, from the PA output node, is 12dB with 6GHz 3-dB bandwidth (Fig. 4 c) and -15dB simulated return loss (S11). A test structure for the same series fed patch antenna [6] shows a measured gain of 11dB and 12° E-plane 3-dB beam width.

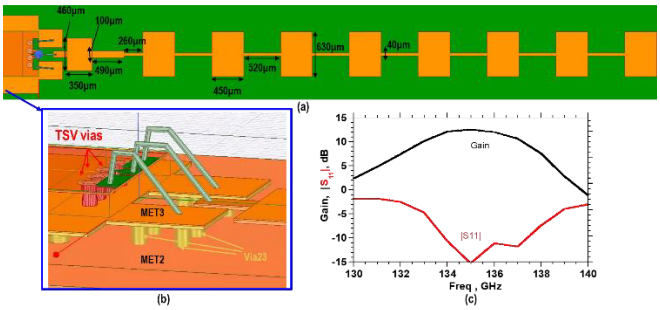

Fig. 4. Series Fed patch antenna (a) Design on HFSS, (b) InP-antenna transition, (c) Simulated antenna gain and return loss, inclusive of the InP-LTCC wire bonds and the matching network.

III. INTEGRATED TRANSMITTER MODULE

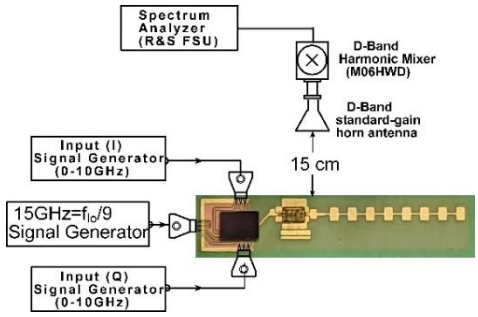

Fig. 5. Integrated transmitter module Gain and EIRP measurement setup

The integrated transmitter module was tested using the setup of Fig. 5. The module conversion gain, and modulation bandwidth were measured at a fixed 135GHz LO frequency, while the baseband (I or Q) signal is swept from 100MHz to 10GHz. The transmitted signal's upper and lower side bands are captured using a D-band harmonic mixer and spectrum analyser calibrated against a power meter. The measurement (Fig. 6a) shows 6GHz 3-dB modulation bandwidth and 36dB conversion gain.

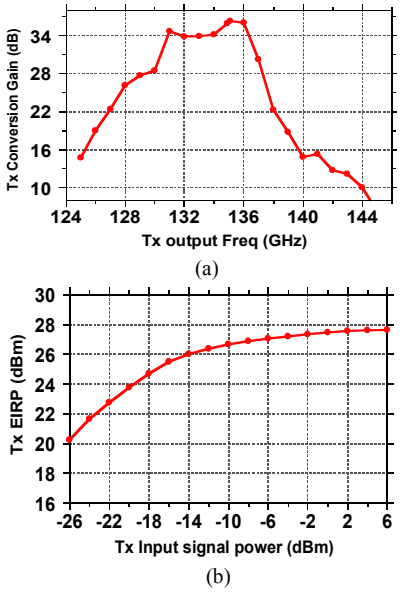

Fig. 6. (a) Transmitter module frequency response (b) Pout Vs Pin characteristic

The saturated EIRP is measured using the same setup, fixing the LO at 135GHz and the baseband signal at 100MHz while sweeping the baseband signal power from -26dBm to 6dBm. The measured saturated EIRP is 27.5dBm (Fig. 6b).

The transmitter's radiation pattern (Fig. 7) was also measured using the setup of Fig. 5 while placing the receiver antenna on a rotating arm and moving it in both elevation and azimuth. The maximum EIRP is at 4 degrees from broadside.

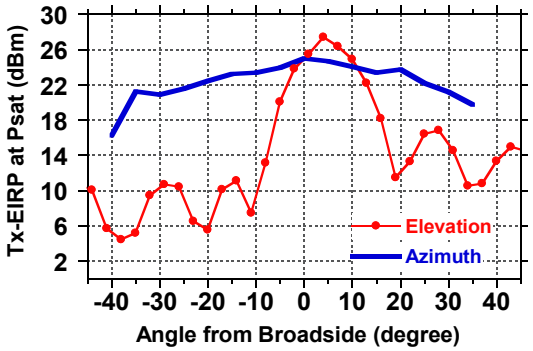

Fig. 7. Module radiation pattern in E &H planes

To test spectral purity, a baseband signal (I or Q) was applied at 1GHz while fixing the LO at 135GHz. The upper and lower sidebands and the LO feedthrough were captured using a harmonic mixer and spectrum analyser (Fig. 8). The LO feedthrough is suppressed by 13dB relative to the LSB.

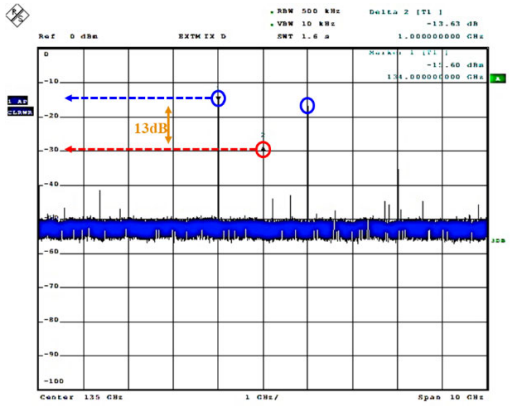

Fig. 8. Integrated transmitter module output spectrum

A. *Transmitter Module Modulation performance*

Modulation performance of the transmitter module was then characterized (Fig. 9) using an arbitrary waveform generator (AWG) for the transmitter input signals, and monitoring the module output at 15cm propagation distance using a horn antenna, a D-band fundamental mixer for frequency down conversion, and a digital storage oscilloscope (DSO) for signal acquisition. The AWG was set to generate different signal constellations modulating a 4GHz IF, with the transmitter module then upconverting this modulated signal to a 134GHz carrier. The D-band fundamental mixer down-converts the received signal to a 4GHz IF. The DSO demodulates the received signal, and, after adaptive equalization, displays (Table 1) the modulation constellation and computes the error vector magnitude (EVM). The stated EVM magnitudes are referenced to the constellation's RMS amplitude. Under 5Gbaud, 64QAM modulation (30Gbps), the module shows 8.5% RMS error vector magnitude (EVM) at 21.5dBm EIRP.

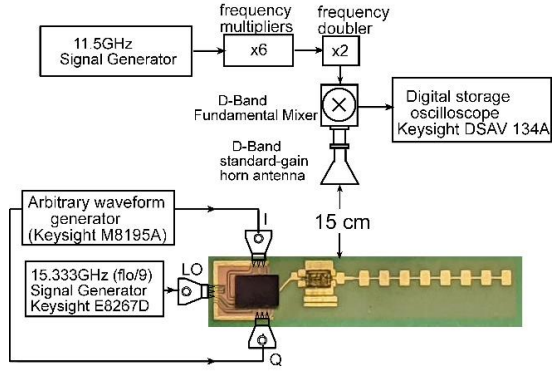

Fig. 9. Transmitter module modulation characterization.

Table. 1. Transmitter module measured modulation constellations and computed error vector magnitudes.

EIRP=24dBm/ 3dB Back off from P_{sat}		
QPSK (1GBaud)	16QAM(1GBaud)	64QAM(1GBaud)
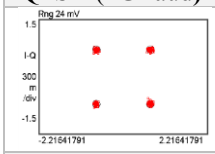	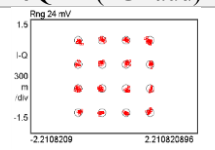	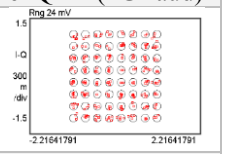
5.4% (RMS)	6.8% (RMS)	6.5% (RMS)
EIRP=21dBm/ 6dB Back off from P_{sat}		
QPSK (5GBaud)	16QAM(5GBaud)	64QAM(5GBaud)
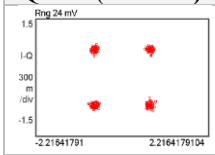	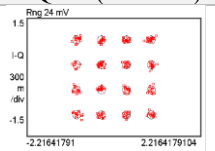	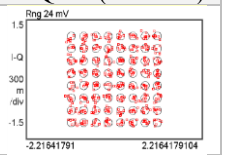
7.69% (RMS)	8.4% (RMS)	8.5% (RMS)

For each of the supported modulation schemes, the RMS error vector magnitude was measured (Fig. 10) at different output power while fixing the data rate at 1GBaud. Similarly, the RMS error vector magnitude was measured as a function of symbol rate at a fixed 21dBm EIRP of 21dBm (Fig. 11).

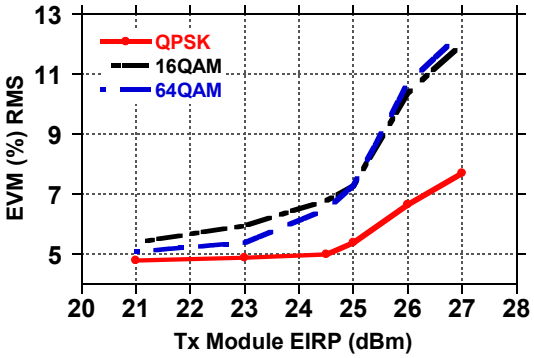

Fig. 10. Transmitter module measured error vector magnitude vs. EIRP for different modulation constellations at 1GBaud symbol rate.

Table. 2. Comparison with state-of-the-art D-band transmitters

	[2]	[3]	[7]	[8]	This Work
Package Technology	Silica based with WR-6 transition	Radio on Glass with WR-6 transition	Radio on PCB (Astra MT77)	No	LTCC Interposer
IC Technology	70nm GaAs mHEMT	0.13µm SiGe-BICMOS	45nm CMOS SOI	0.25µm InP DHBT	22nm FDSOI + 0.25µm InP HBT
Antenna Integration	No	No	Antenna on PCB	No	Antenna on Ceramic carrier
Frequency (GHz)	142-157	115-155 (LB) 135-170 (HB)	142-147	110-160	131-137
Tx Gain	12dB	17dB (LB) 18dB (HB)	NA	24dB	36dB
EIRP (dBm) at Psat	-	-	14dBm	-	27.5dBm
Tx-Psat	8dBm	13dBm	2dBm	9dBm	17dBm*
Tx Pdc (mW)	1100	1350 (LB) 2100 (HB)	-	170	760
Tx Peak data rate/ Modulation	10Gb/s (128QAM) EVM (N/A)	42-Gb/s (128-QAM) EVM (4.4%)	10Gb/s (QPSK) EVM (NA)	20-Gb/s^{++} 32QAM EVM (10.6%)	30Gb/s (64QAM) EVM-RMS (8.5%)
P_{out} at Peak data rate	NA	0.5dBm	2dBm	NA	11dBm*

*calculated as (EIRP-antenna gain), $^{++}$ Link include Tx and RX ** EIRP from combing two transmitter channels

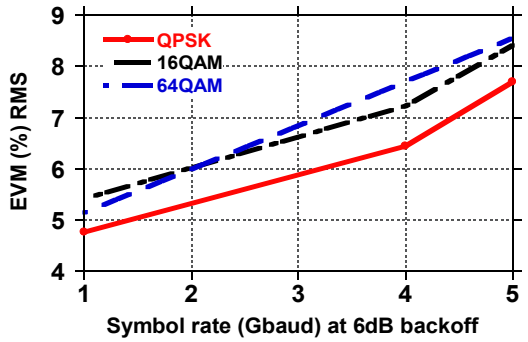

Fig. 11. Transmitter module measured error vector magnitude vs. symbol rate for different modulation constellations at 21dBm EIRP.

The integrated transmitter module consumes 760mW (200mW in the CMOS transmitter and 560mW in the InP PA). Table 2 compares the transmitter module with recent published packaged modules in D-band.

IV. Conclusion

This paper presents a D-band transmitter module, packaged on a low-permittivity Kyocera LTCC carrier (GL771). The integrated transmitter module has 6GHz 3-dB modulation bandwidth and, under 5Gbaud, 64QAM modulation (30Gbps), shows 8.5% RMS error vector magnitude (EVM) at 21.5dBm EIRP. The measured EIRP is 27.5dBm at P_{sat}, which is to the authors' knowledge the highest reported EIRP from a packaged single channel transmitter module at D-band.

Acknowledgment

This work was supported in part by the Semiconductor Research Corporation (SRC) under the JUMP program (2018-JU-2778) and by DARPA (HR0011-18-3-0004). Authors are so grateful for Kyocera for the ceramic carrier fabrication and for Kyocera San Diego for all the assembly efforts. Authors would like to thank GlobalFoundries for the 22nm FDSOI chip fabrication.

References

[1] A. A. Farid, A. Simsek, A. S. H. Ahmed and M. J. W. Rodwell, "A Broadband Direct Conversion Transmitter/Receiver at D-band Using CMOS 22nm FDSOI," 2019 IEEE Radio Frequency Integrated Circuits Symposium (RFIC), Boston, MA, USA, 2019, pp. 135-138

[2] M. Ito, T. Okawa and T. Marumoto, "D-band Transceiver Utilizing 70-nm GaAs-mHEMT Technology for FDD System," 2019 IEEE BiCMOS and Compound semiconductor Integrated Circuits and Technology Symposium (BCICTS), Nashville, TN, USA, 2019, pp. 1-4

[3] A. Singh et al., "A D-Band Radio-on-Glass Module for Spectrally-Efficient and Low-Cost Wireless Backhaul," 2020 IEEE Radio Frequency Integrated Circuits Symposium (RFIC), Los Angeles, CA, USA, 2020, pp. 99-102

[4] A. S. H. Ahmed, A. Simsek, A. A. Farid, A. D. Carter, M. Urteaga and M. J. W. Rodwell, "A W-Band transmitter channel with 16dBm output power and a receiver channel with 58.6mW DC power consumption using heterogeneously integrated InP HBT and Si CMOS technologies," 2019 IEEE MTT-S International Microwave Symposium (IMS), Boston, MA, USA, 2019, pp. 654-657

[5] A. S. H. Ahmed, M. Seo, A. A. Farid, M. Urteaga, J. F. Buckwalter and M. J. W. Rodwell, "A 140GHz power amplifier with 20.5dBm output power and 20.8% PAE in 250-nm InP HBT technology," 2020 IEEE/MTT-S International Microwave Symposium (IMS), Los Angeles, CA, USA, 2020, pp. 492-495

[6] A. A. Farid, A. S. H. Ahmed, A. Simsek and M. J. W. Rodwell, " A Packaged 135GHz 22nm FD-SOI Transmitter on an LTCC Carrier," IEEE/MTT-S International Microwave Symposium (IMS), Atlanta, GA, USA, 2021

[7] A. Simsek, A. S. H. Ahmed, A. A. Farid, U. Soylu and M. J. W. Rodwell, "A 140GHz Two-Channel CMOS Transmitter Using Low-Cost Packaging Technologies," 2020 IEEE Wireless Communications and Networking Conference Workshops (WCNCW), Seoul, Korea (South), 2020, pp. 1-3

[8] S. Carpenter, D. Nopchinda, M. Abbasi, Z. S. He, M. Bao, T. Eriksson, and H. Zirath, "A D-Band 48-Gbit/s 64-QAM/QPSK Direct-Conversion I/Q Transceiver Chipset," IEEE Transactions on Microwave Theory and Techniques, vol. 64, no. 4, pp. 1285–1296, April 2016.